Chemistry–A European Journal
Research Article
doi.org/10.1002/chem.202201473
Chemistry Europe
European Chemical Societies Publishing
www.chemeurj.org

An Anionic Amido-Substituted Seven-Vertex Siliconoid Cluster

Jan Keuter,[a] Maria Dimitrova,[b] Oliver Janka,[a] Alexander Hepp,[a] Raphael J. F. Berger,*[b] and Felicitas Lips*[a]

Abstract: The silanide $[Si_4\{N(SiMe_3)Dipp\}_3]^-$ (**1**) transforms into the anionic siliconoid cluster $[Si_7\{N(SiMe_3)Dipp\}_3]^-$ (**2**) with four unsubstituted silicon atoms as a contact ion pair with [K([18]crown-6)] in C_6D_6 at room temperature within five weeks. Anion **2** was investigated by natural population analysis and visualization of intrinsic atomic orbitals. Magnetically induced current-density calculations of **2** revealed two distinct strong diatropic vortices that sum up in one direction and create a strongly shielded apical silicon atom in **2**.

When reasonings based on Lewis structures fail to describe the stability of classes of compounds such as main-group metal clusters, arguments about their aromaticity are often made.[1] Hirsch developed the $2(N+1)^2$ electron counting rule to determine the aromaticity of fullerenes.[2] This concept can also be applied to highly symmetric polyhedral boranes, and it was extended to Zintl clusters that can usually also be described by applying the Wade–Mingos rules.[3,4] In this regard, the concept of spherical aromaticity[5] is used to describe the unusual stability, structure, bonding and nuclear magnetic shielding that is present, for instance, in $[Si_4]^{4-}$ and P_4. Furthermore, the magnetic criterion for aromaticity[6] is used and either determined experimentally by NMR chemical shifts or computationally with quantum chemistry methods by calculating magnetically induced current densities.[7] The latter method is applied to analyze and visualize the magnetic anisotropy in siliconoid clusters.[8] This type of clusters, named in analogy to metalloid clusters,[9] includes partially substituted silicon clusters with at least one hemispheroidal silicon atom that bears no substituents. At the hemispheroidal, unsubstituted silicon atom all bonds point into one hemisphere. These positions in silicon clusters were previously described as inverted tetrahedral.[10] In contrast to Zintl anions, electron counting rules for metalloid and siliconoid clusters are usually less clear.

The unsubstituted silicon atoms in siliconoids display upfield-shifted ^{29}Si NMR chemical shifts similar to those observed for Zintl anions. In addition to the strongly shielded silicon atoms in siliconoids, signals shifted in the downfield region are reported. For instance, for a siliconoid named benzpolarene, this results in a difference of $\Delta\delta = 448.8$ ppm in chemical shifts between these different types of positions..[11]

Upon calculation of the magnetically induced current density of the cluster, the wide distribution of chemical shifts and electronic anisotropy was rationalized. This method was applied to the benzpolarene siliconoid cluster and a hexasilabenzene isomer[12] and showed the presence of a diamagnetic vortex but no paramagnetic contribution to the total current density. The strong upfield shift at the hemispheroidal silicon atoms is created by a diatropic current vortex that induces a strong shielding effect at these positions. Overall, the situation in these siliconoids is similar to spherical aromatic inorganic compounds such as P_4.

The current focus in the field of siliconoid clusters is to increase the number of unsubstituted atoms in these compounds and to succesfully synthesize derivatives with main-group and/or transition metal units.[13] The latter was achieved by the selective cleavage of one substituent from tetrasilatetrahedranes leading to anionic clusters such as $[Si_4R_3]^-$ **A** shown in Figure 1 ($R = SiMe\{CH(SiMe_3)_2\}_2$ and $R = SitBu_3$).[14] Cleavage of one substituent from the benzpolarene leads to $[Si_6Tip_5]^-$ **B** (Tip = 2,4,6-tri*iso*propylphenyl)[15] that can be used in salt metathesis reactions to introduce functional groups (Figure 1). This strategy was extended to site-selective functionalization upon cleavage of a different substituent from the original benzpolarene cluster to obtain **C**,[16] and to mixed group 14 metalloid clusters to yield **D** (Figure 1).[17]

Moreover, the use of Zintl anions such as $[Si_4]^{4-}$ and $[Si_9]^{4-}$ as precursors in the reaction with mesityl copper,[18] $ZhPh_2$,[19] $NiCO_2(PPh_3)_2$[20] and transition metal NHC units allows the formation of anionic substituted silicon clusters with ligand-free atoms.[21] For instance, the number of unsubstituted atoms was increased by the successful introduction of silyl groups to the Zintl anion $[Si_9]^{4-}$, resulting in anionic clusters **E** and **F** with a

[a] Dr. J. Keuter, Dr. O. Janka, Dr. A. Hepp, Dr. F. Lips
Westfälische Wilhelms-Universität Münster
Institut für Anorganische und Analytische Chemie
Corrensstraße 28–30, 48149 Münster (Germany)
E-mail: lips@uni-muenster.de

[b] M. Dimitrova, Priv. Doz. Dr. R. J. F. Berger
Paris-Lodron Universität Salzburg, Materialchemie
Jakob-Harringerstr. 2a, 5020 Salzburg (Austria)
E-mail: Raphael.Berger@sbg.ac.at

Supporting information for this article is available on the WWW under https://doi.org/10.1002/chem.202201473

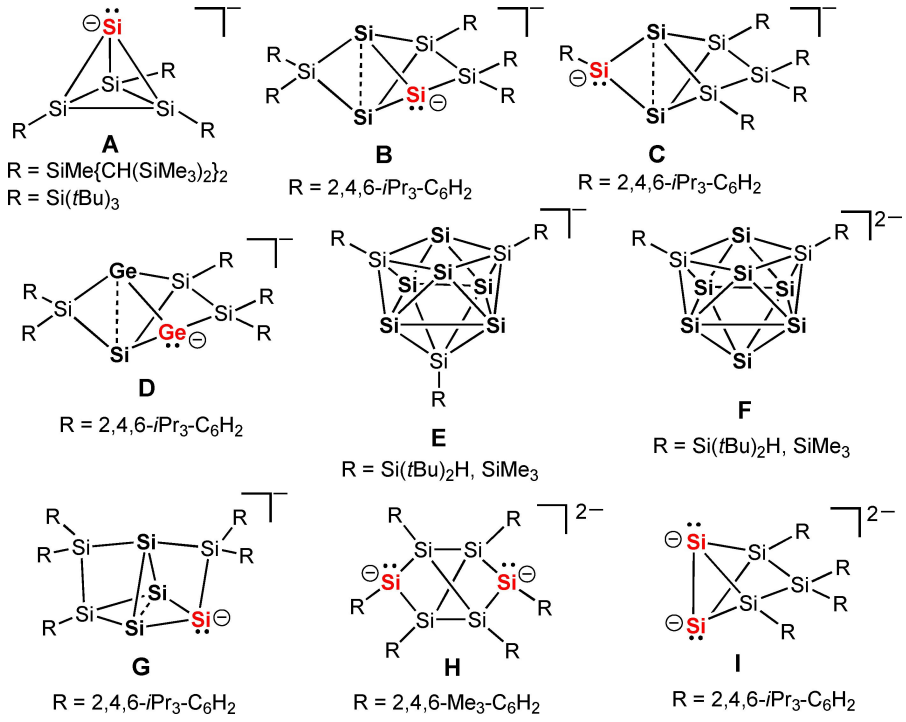

Figure 1. Anionic silicon clusters. Atoms highlighted in red represent the anionic sites that are coordinated by cations.

high number of six and seven unsubstituted silicon atoms, respectively (Figure 1).[22]

Furthermore, an anionic cluster with four unsubstituted silicon atoms **G** was obtained in an atomically precise expansion of unsaturated silicon clusters.[23] Recently, also a dianionic six-vertex cluster $[Si_6R_6]^{2-}$ **H** (R = 2,4,6-trimethylphenyl) was reported as a [K([18]crown-6)(DME)] salt (DME = 1,2-dimethoxyethane) and used in redox reactions with transition metal compounds (Figure 1).[24] The dianionic silicon cluster **I** depicted in Figure 1 was obtained by the selective removal of a SiR_2 unit from a siliconoid cluster and functionalized with organoboryl and phosphane groups.[25]

In this work, we abstracted one amido substituent from the bicyclic silicon(I) ring compound **J**[26a] with KC_8 in the presence of [18]crown-6 in THF at −78 to −30 °C in 15 h. This generated the anionic substituted four-vertex silicon ring compound **1** after filtration and concentration of the green solution at −30 °C and subsequent layering with cold *n*-hexane at −32 °C in form of single crystals.[26b] In the present case, the green solution was evaporated to dryness and the green solid was suspended into benzene at room temperature. After storage of this solution for five weeks at room temperature, the seven-vertex anionic cluster [K([18]crown-6)][Si_7{N($SiMe_3$)Dipp}$_3$] **2** with four unsubstituted silicon atoms was isolated in low yield of 7% in form of red single crystals, which is illustrated in Scheme 1.[27] Within five weeks, the formation of **2** was monitored using time-dependent NMR spectroscopy (Figures S13 and S14 in the Supporting Information). But the assignment of the signals in the ^{29}Si NMR spectra to any intermediate of the process was not possible. Hence, no clear suggestion about the formation mechanism of **2** can be given at this point.

The anion in **2** has the shape of a mono-capped octahedron. The upper three-membered, amido-substituted Si_3 ring composed of Si2, Si3 and Si4 is capped by the unsubstituted Si1 atom and connected to a lower three-membered ring composed of the ligand-free silicon atoms Si5, Si6, and Si7 (Figure 2). The bond lengths from the apical Si1 atom to the amido-substituted silicon atoms Si2, Si3, Si4 (2.346(3)–2.348(0) Å) are in the range of Si–Si single bonds (2.34 Å). The distances within the amido-substituted silicon atoms are significantly elongated (2.618(8)–2.660(8) Å) compared to single bonds. The bond lengths from Si2-4 to Si5-7, that is, those from the substituted Si_3 ring to the lower unsubstituted Si_3 ring, alternately change from single (2.371(8)–2.374(8) Å) to strongly elongated single bonds (2.450(8)–2.505(8) Å). The bond lengths in the lower unsubstituted three-membered silicon ring range from 2.474(8)–2.483(8) Å and are also longer than a usual Si–Si bond of 2.34 Å. Elongated bond lengths due to coordination numbers higher than four and multicenter bonds were also observed in the silyl-substituted nine-vertex silicon clusters (2.405(2)–2.782(2) Å).[22] In **2**, the silicon atoms in the lower ligand-free Si_3 ring have contacts to the K([18]crown-6) counterion. The distances of Si5–Si7 to K1 (3.557(2)–3.602(1) Å) are longer than the sum of the covalent radii of K and Si (3.38 Å) and in the upper range of those observed in potassium silanides (3.30–3.58 Å).[28] A similar shorter Si···K distance (3.291 Å) was found in [K[18]crown-6][Si_4($SitBu_3$)$_3$].[14b] By contrast, in the crystal structure, the apical Si1 atoms display distances to the potassium cations that are significantly longer

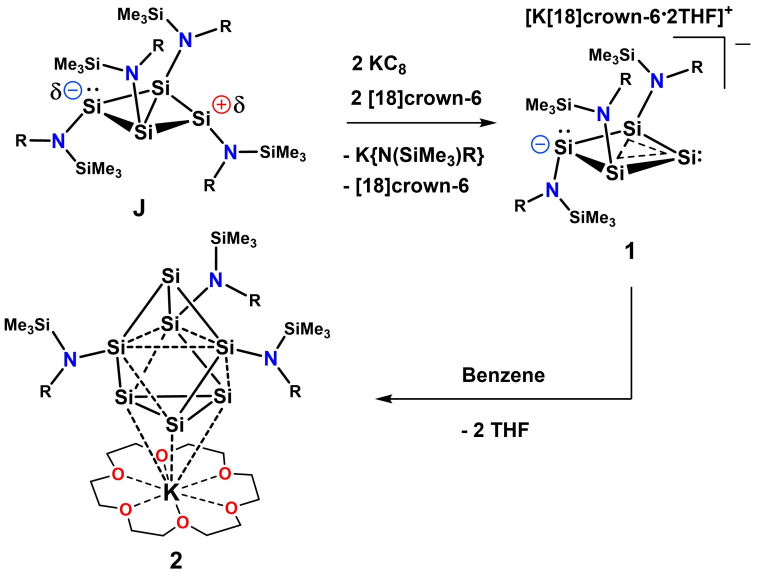

Scheme 1. Synthesis of **2** (R = 2,6-diisopropylphenyl).

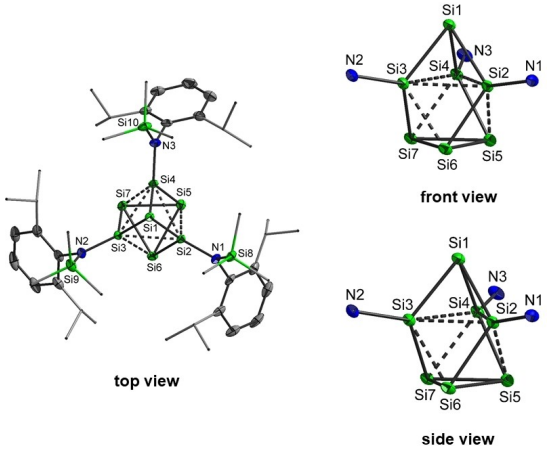

Figure 2. Left: Top view of the molecular structure of the anion in **2**. Right: Cut-out of the cluster core of the anion in **2** in two different views. Thermal ellipsoids are set at the 50% probability level. H atoms are not shown. The isopropyl and $SiMe_3$ groups of the {N(SiMe$_3$)Dipp} substituents are represented as wires for clarity. Selected bond lengths/Å: Si1–Si2 2.348(1), Si1–Si3 2.347(2), Si1–Si4 2.346(1), Si2–Si3 2.660(1), Si3–Si4 2.639(1), Si2–Si4 2.618(1), Si2–Si5 2.502(1), Si2–Si6 2.372(1), Si3–Si6 2.505(1), Si3–Si7 2.374(1), Si4–Si5 2.371(1), Si4–Si7 2.450(1), Si5–Si6 2.482(1), Si5–Si7 2.474(1), Si6–Si7 2.483(1), Si2–N1 1.742(2), Si3–N2 1.745(2), Si4–N3 1.741(2), Si8–N1 1.761(2), Si9–N2 1.760(2), Si10–N3 1.757(2).

with 6.171(3) and 6.234(2) Å for the two independent molecules of **2** (see the Supporting Information).

Compound **2** does not dissolve in C_6D_6 but it is soluble in [D_8]THF. In this solvent, one set of signals for the amido substituents appears and three signals for the chemically and magnetically different silicon atoms of the cluster core at +113.2, −82.9 and −413.8 ppm. These measured chemical shifts correlate well with the calculated chemical shifts of the contact ion pair, indicating that the coordination to [K(18-crown-6)]$^+$ may persist even in the coordinating solvent THF. The dissociation of the contact ion pair in separate ions was calculated to require 14.2 kcal/mol. This confirms the high stability of **2** even in THF.

The signal at +113.2 ppm in the ^{29}Si NMR spectrum in [D_8]THF is assigned to the amido-substituted silicon atoms (Si2, Si3 and Si4). The resonance at −82.9 ppm is attributed to the three unsubstituted silicon atoms (Si5, Si6 and Si7) coordinated by [K[18]crown-6)]$^+$, and the signal at −413.8 ppm belongs to the unsubstituted apical Si1 atom. In comparison to previously reported anionic siliconoid clusters, the signal of Si1 is, to the best of our knowledge, the most shielded silicon atom in this class of compounds. For [K-222-crypt][(Si(*t*Bu)$_2$H)$_3$Si$_9$][22a] a signal at −358 ppm was recorded and for [Li([12]crown−4)$_2$][Si$_6$Tip$_5$][15] signals at −230.9 and −232.6 ppm were found. The resonance appears at even higher field than that of the protonated Zintl anion [Si_4H]$^{3-}$ in liquid ammonia (−327.8 and −404.5 ppm).[29] Furthermore, in the anion in **2**, the apical silicon atom and the adjacent amido-substituted silicon atoms feature a very large difference in their chemical shifts of $\Delta\delta = 527$ ppm. This extreme difference was not observed in siliconoids before, but it is typical for siliconoids which feature remarkable electronic anisotropy. For the Zintl anion [Si_5]$^{2-}$ a difference in chemical shift between adjacent silicon atoms of $\Delta\delta = 696.5$ ppm was reported.[29]

The extremely high-field shift of the resonance for Si1 might be related to the accumulation of negative charge at this position. Indeed, according to natural population analysis (NPA) in the model anion without the coordination of [K([18]crown-6)]$^+$, the apical Si1 atom (−0.50) displays a more negative partial charge than the other unsubstituted silicon atoms of the lower three−membered ring (−0.18). The amido-substituted silicon atoms feature positive partial charges of 0.62. Thus, the difference in the partial charges between the apical Si1 atom and the neighboring amido-substituted silicon atoms (Si2, Si3 and Si4) is 1.12. This difference is much larger than that for the

silicon atoms (0.50 and 0.62) in the unsaturated charge-separated planar four-membered silicon ring compounds $Si_4(Emind)_4$ and $Si_4\{N(SiMe_3)_2\}_4$.[30]

Compound **2** was further analyzed with DFT calculations at the TPSS-D3(BJ)/def2-TZVP level of theory.[31–33] The frontier molecular orbitals of the anion in **2** display delocalized multi-center bonds (Figure S21). Calculated intrinsic atomic orbitals (IAOs)[34] show 2c–2e bonds from the apical Si1 atom to the amido-substituted silicon atoms. Furthermore, this type of bond is also present in the short Si2–Si6, Si3–Si7 and Si4–Si5 bonds. Lone pairs of electrons were assigned to Si1 and the unsubstituted silicon atoms Si5, Si6 and Si7. In addition, three IAOs represent multicenter bonds. Each of these IAOs includes two silicon atoms of the amido-substituted Si_3 ring and two of the lower ligand-free Si_3 ring (Figure S22).

The anion in **2** is a main-group cluster species which might suggest to naively apply the Wade-Mingos rules (WM)[3,4] to explain its structure and properties. The seven-vertex cluster ($n=7$) possesses 18 skeletal electrons, which correspond to nine electron pairs. Thus, the cluster electron count rule yields $9=n+2$ electron pairs for the anion in **2**. Hence, this species is predicted to be a *nido*-cluster in the framework of WM rules. The corresponding borane reference cluster, B_7H_{11}, is a *nido*-snub disphenoid, which is in marked contrast to the observed structure of **2**. However, the most regular 8-vertex polyhedron is a cube, hence, we suggest interpreting this structure as a (distorted) *nido*-cube (or a *nido*-rhombus for that matter), with the unoccupied vertex space diagonally opposing Si1. Alternatively, a potassium ion can be integrated into the model as a cluster atom, and then the predicted position coincides precisely with the observed one, while also the cluster anion becomes a neutral *closo*-cluster. In agreement with this slightly modified WM interpretation (by modifying the base polyhedron) of the anion in **2**, one would expect properties typical for 3D-aromatic systems.[5] Thus we have undertaken an in-depth analysis of the magnetic response properties of **2**, to determine the degree of spherical aromaticity.

The experimental determination of the magnetic susceptibility of salt **2** depicted in Figure S23 did not show significant temperature dependence and resulted in a value of $-1.7\times10^{-8}\,m^3\,mol^{-1}$ which is not in contradiction to the isotropic value of $-2.3\times10^{-8}\,m^3\,mol^{-1}$ calculated for the isolated anion of **2**. This confirms the diamagnetic properties of **2** as expected on the basis of WM descriptions.

Additionally, we performed magnetically induced current-density calculations (MICD) on a simplified model cluster anion $[Si_7(NH_2)_3]^-$ at the density functional theory (DFT) level of theory (TPSS-D3(BJ)/def2-TZVP, see page S32). The magnetically induced electronic current-density field can be interpreted as a field of induced electron mobility, and it is closely related to electron delocalization.[7] With this analysis, we tried to address two questions:

1) How strong is the diamagnetic current-density response of the anion in **2**?
2) How significantly does this response depend on the direction of the external magnetic field?

A closer inspection of the MICD in $[Si_7(NH_2)_3]^-$ shows that it can be partitioned into two separate vortex regions in the molecule. The first domain is located in the spatial region surrounding the apical Si1 atom and the other one is located around the remaining six Si atoms. They are shown in Figures 3 and 4 and were labeled as loop β and loop γ, respectively.

The global outermost current-density domain, which the cluster is embedded in, is labeled as loop α. Due to the C_{3v} symmetry of the anion, the first-order magnetic response is uniquely characterized by applying the field in two directions (the magnetic susceptibility tensor has two degenerate principal axes). We chose symmetry axis z as one magnetic field direction and the x Cartesian axis perpendicular to the z-axis for the other. The total flux (= integrated MICD) for the valence electron contributions (see Figures S25–S28 for the integration procedure) amounts to $31.6\,nA\,T^{-1}$ if the external magnetic field ($\mathbf{B}^{ext}$) is parallel to z ($\mathbf{B}_z$) and $29.8\,nA\,T^{-1}$ for $\mathbf{B}_x$. This is in agreement with the comparably small differences in the calculated magnetic susceptibilities for $\mathbf{B}_z$ of $-2.5\times10^{-8}\,m^3\,mol^{-1}$ and with $\mathbf{B}_x$ of $-2.2\times10^{-8}\,m^3\,mol^{-1}$.

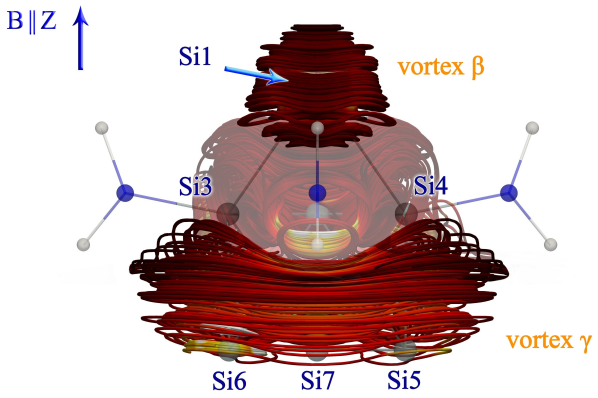

Figure 3. Plot of the calculated magnetically induced current density of the model compound $[Si_7(NH_2)_3]^-$. Current density for the external field parallel to the z-axis.

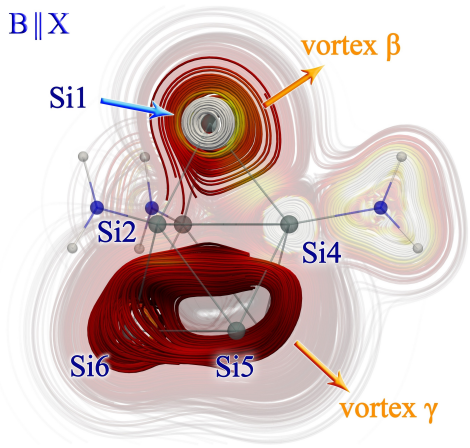

Figure 4. Plot of the calculated magnetically induced current density of the model compound $[Si_7(NH_2)_3]^-$. Current density for the external field parallel to the x-axis.

Thus, in agreement with the model of a 3D aromatic system implied by the applicability of WM rules, the magnetic response shows a considerable tendency towards isotropy. However, in contradiction to this, there is no single homogeneous current vortex domain but two different domains. In the case of $\mathbf{B}_z$, the two domains are merged on top of each other such that they act as one strong diatropic vortex that yields the extreme shielding of Si1 in the ^{29}Si NMR spectrum at −413.8 ppm while for other orientations of $\mathbf{B}^{ext}$, especially along the *x* and *y* directions, the vortices are separated as distinct domains (Figures 3 and 4).

An attempt to numerically quantify the two domains for $\mathbf{B}_x$ yields 11.6 nA T^{-1} for the Si1-centered current vortex and 17.0 nA T^{-1} for the current in the remaining Si_6 scaffold, whereas for $\mathbf{B}_z$ the corresponding integrated current strengths are 9.1 and 17.7 nA T^{-1}, respectively. In both cases the vortices are strongly diatropic. For comparison, benzene shows a net magnetically induced current of 12.6 nA T^{-1} (diatropic) at this level of theory, which confirms the aromatic nature of the cluster anion according to the magnetic criterion for aromaticity.[6]

Furthermore, we compared the situation in **2** with the magnetic response current density of the benzpolarene Si_6Tip_6 which can formally be interpreted as the global minimum conformer of hexasilabenzene.[11] Intriguingly, also in this cluster, the current-density field appears to be composed of two roughly separable components. Unlike in this case one of the two apical Tip_2Si (non-cluster) current field components of Si_6Tip_6 is of a distinct paratropic nature, while the remaining (cluster) current component shows a clear diatropicity.[11] At this stage it would be highly speculative to draw further conclusions, but it seems worthwhile to at least note the observation of the existence of two apparently separable current domains in each of the two siliconoids, **2** and Si_6Tip_6.

In summary, we have described a unique seven-vertex, amido-substituted, anionic siliconoid cluster with four unsubstituted silicon atoms that displays a resonance at a record upfield chemical shift of −413.8 ppm for the apical silicon atom. Analysis of the calculated current density revealed two distinct strongly diatropic vortices that sum up in one direction and create the highly shielded situation.

Acknowledgements

We thank the DFG (Heisenberg Programm to F.L. LI3087/2-1) for financial support and Profs. W. Uhl and F. E. Hahn for generous support. The theoretical and computational group of Prof. D. Sundholm at the University of Helsinki is acknowledged for the computational resources. M.D. thanks the Finnish Cultural Foundation for a research grant. Open Access funding enabled and organized by Projekt DEAL.

Conflict of Interest

The authors declare no conflict of interest.

Data Availability Statement

The data that support the findings of this study are available in the supplementary material of this article.

Keywords: aromaticity · clusters · N ligands · silicon · siliconoids

[1] S. Dehnen, *Clusters: Contemporary Insight in Structure and Bonding*, Springer International, **2017**.
[2] A. Hirsch, Z. Chen, H. Jiao, *Angew. Chem. Int. Ed.* **2001**, *40*, 2834–2838; *Angew. Chem.* **2001**, *113*, 2916–2920.
[3] a) K. Wade, *Adv. Inorg. Chem. Radiochem.* **1976**, *18*, 1–67; b) D. M. P. Mingos, *Nat. Phys. Sci.* **1972**, *236*, 99–102;
[4] a) D. M. P. Mingos *Acc. Chem. Res.* **1984** *17*, 311–319; b) K. Wade *J. Chem. Soc. D* **1971**, 792–793.
[5] a) R. B. King, *Chem. Rev.* **2001**, *101*, 1119–1152; b) Z. Chen, R. B. King, *Chem. Rev.* **2005**, *105*, 3613–3642; c) A. Hirsch, Z. Chen, H. Jiao, *Angew. Chem. Int. Ed.* **2000**, *39*, 3915–3917; *Angew. Chem.* **2000**, *112*, 4079–4081; d) J. Poater, C. Viñas, I. Bennour, S. Escayola, M. Solà, F. Teixidor *J. Am. Chem. Soc.* **2020**, *142*, 9396–9407.
[6] a) R. Gershoni-Poranne, A. Stanger, *Chem. Soc. Rev.* **2015**, *44*, 6597–6615; b) V. I. Minkin, *Pure Appl. Chem.* **1999**, *71*, 1919–1981.
[7] D. Sundholm, H. Fliegl, R. J. Berger, *Wiley Interdiscip. Rev.: Comput. Mol. Sci.* **2016**, *6*, 639–678.
[8] a) Y. Heider, D. Scheschkewitz, *Chem. Rev.* **2021**, *121*, 9674–9718; b) Y. Heider, D. Scheschkewitz, *Dalton Trans.* **2018**, *47*, 7104–7112.
[9] A. Schnepf, *Chem. Soc. Rev.* **2007**, *36*, 745–758.
[10] T. Iwamoto, S. Ishida, *Chem. Lett.* **2014**, *43*, 164–170.
[11] K. Abersfelder, A. J. P. White, R. J. F. Berger, H. S. Rzepa, D. Scheschkewitz, *Angew. Chem. Int. Ed.* **2011**, *50*, 7936–7939; *Angew. Chem.* **2011**, *123*, 8082–8086.
[12] R. J. F. Berger, H. S. Rzepa, D. Scheschkewitz, *Angew. Chem. Int. Ed.* **2010**, *49*, 10006-10009; *Angew. Chem.* **2010**, *122*, 10203–10206.
[13] a) N. E. Poitiers, V. Huch, M. Zimmer, D. Scheschkewitz, *Chem. Eur. J.* **2020**, *26*, 16599–16602; b) N. E. Poitiers, L. Giarrana, V. Huch, M. Zimmer, D. Scheschkewitz, *Chem. Sci.* **2020**, *11*, 7782–7788; c) N. E. Poitiers, V. Huch, M. Zimmer, D. Scheschkewitz, *Chem. Commun.* **2020**, *56*, 10898–10901; d) N. E. Poitiers, L. Giarrana, K. I. Leszczyńska, V. Huch, M. Zimmer, D. Scheschkewitz, *Angew. Chem. Int. Ed.* **2020**, *59*, 8532–8536; *Angew. Chem.* **2020**, *132*, 8610–8614.
[14] a) M. Ichinohe, M. Toyoshima, R. Kinjo, A. Sekiguchi, *J. Am. Chem. Soc.* **2003**, *125*, 13328–13329; b) T. M. Klapötke, S. Kumar Vasisht, G. Fischer, P. Mayer, *J. Organomet. Chem.* **2010**, *695*, 667–672.
[15] P. Willmes, K. Leszczyńska, Y. Heider, K. Abersfelder, M. Zimmer, V. Huch, D. Scheschkewitz, *Angew. Chem. Int. Ed.* **2016**, *55*, 2907–2910; *Angew. Chem.* **2016**, *128*, 2959–2963.
[16] Y. Heider, N. E. Poitiers, P. Willmes, K. I. Leszczyńska, V. Huch, D. Scheschkewitz, *Chem. Sci.* **2019**, *10*, 4523–4530.
[17] L. Klemmer, V. Huch, A. Jana, D. Scheschkewitz, *Chem. Commun.* **2019**, *55*, 10100–10103.
[18] M. Waibel, F. Kraus, S. Scharfe, B. Wahl, T. F. Fässler, *Angew. Chem. Int. Ed.* **2010**, *49*, 6611-6615; *Angew. Chem.* **2010**, *122*, 6761–6765.
[19] J. M. Goicoechea, S. C. Sevov, *Organometallics* **2006**, *25*, 4530–4536.
[20] S. Joseph, M. Hamberger, F. Mutzbauer, O. Härtl, M. Meier, N. Korber, *Angew. Chem. Int. Ed.* **2009**, *48*, 8770–8772; *Angew. Chem.* **2009**, *121*, 8926–8929.
[21] F. S. Geitner, T. F. Fässler, *Chem. Commun.* **2017**, *53*, 12974–12977.
[22] a) L. J. Schiegerl, A. J. Karttunen, W. Klein, T. F. Fässler, *Chem. Eur. J.* **2018**, *24*, 19171–19174; b) L. J. Schiegerl, A. J. Karttunen, W. Klein, T. F. Fässler, *Chem. Sci.* **2019**, *10*, 9130–9139.
[23] K. Leszczyńska, V. Huch, C. Präsang, J. Schwabedissen, R. J. F. Berger, D. Scheschkewitz, *Angew. Chem. Int. Ed.* **2019**, *58*, 5124–5128; *Angew. Chem.* **2019**, *131*, 5178–5182.
[24] Y. Li, J. Li, J. Zhang, H. Song, C. Cui, *J. Am. Chem. Soc.* **2018**, *140*, 1219–1222.
[25] Y. Heider, P. Willmes, V. Huch, M. Zimmer, D. Scheschkewitz, *J. Am. Chem. Soc.* **2019**, *141*, 19498–19504.
[26] a) J. Keuter, K. Schwedtmann, A. Hepp, K. Bergander, O. Janka, C. Doerenkamp, H. Eckert, C. Mück-Lichtenfeld, F. Lips, *Angew. Chem.* Int. Ed. **2017**, *56*, 13866–13871; *Angew. Chem.* **2017**, *129*, 14054–14059; b) J. Keuter, A. Hepp, A. Massolle, J. Neugebauer, C. Mück-Lichtenfeld, F.

Lips, *Angew. Chem. Int. Ed.* **2022**, *61*, e202114485; *Angew. Chem.* **2022**, *134*, e202114485.
[27] Deposition Number 2172360 contains the supplementary crystallographic data for this paper. These data are provided free of charge by the joint Cambridge Crystallographic Data Centre and Fachinformationszentrum Karlsruhe Access Structures service.
[28] a) D. M. Jenkins, W. Teng, U. Englich, D. Stone, K. Ruhland-Senge, *Organometallics* **2001**, *20*, 4600–4605; b) P. R. Likhar, M. Zimgast, J. Baumgartner, C. Marschner, *Chem. Commun.* **2004**, 1764–1765; c) C. Kayser, R. Fischer, J. Baumgartner, C. Marschner, *Organometallics* **2002**, *21*, 1023–1030.
[29] F. Hastreiter, C. Lorenz, J. Hioe, S. Gärtner, N. Lokesh, N. Korber, R. M. Gschwind, *Angew. Chem. Int. Ed.* **2019**, *58*, 3133–3137; *Angew. Chem.* **2019**, *131*, 3165–3169.
[30] a) K. Suzuki, T. Matsuo, D. Hashizume, H. Fueno, K. Tanaka, K. Tamao, *Science* **2011**, *331*, 1306–1309; b) J. Keuter, A. Hepp, C. G. Daniliuc, M. Feldt, F. Lips, *Angew. Chem. Int. Ed.* **2021**, *60*, 21761–21766; *Angew. Chem.* **2021**, *133*, 21929–21934.
[31] a) R. Ahlrichs, *Phys. Chem. Chem. Phys.* **2004**, *6*, 5119–5121. S. Grimme, J. Antony, S. Ehrlich, H. Krieg, *J. Chem. Phys.* **2010**, *132*, 154104, 1–19; b) S. Grimme, S. Ehrlich, L. Goerigk, *J. Comput. Chem.* **2011**, *32*, 1456–1465.
[32] F. Weigend, R. Ahlrichs, *Phys. Chem. Chem. Phys.* **2005**, *7*, 3297–3305.
[33] a) V. N. Staroverov, G. E. Scuseria, J. Tao, J. P. Perdew, *J. Chem. Phys.* **2004**, *121*, 11507–11507 J; b) J. Tao, J. P. Perdew, V. N. Staroverov, G. E. Scuseria, *Phys. Rev. Lett.* **2003**, *91*, 146401, 1–4.
[34] a) G. Knizia, *J. Chem. Theory Comput.* **2013**, *9*, 4834–4843; b) G. Knizia, J. E. M. N. Klein, *Angew. Chem. Int. Ed.* **2015**, *54*, 5518-5522; *Angew. Chem.* **2015**, *127*, 5609–5613.

Manuscript received: May 12, 2022
Accepted manuscript online: June 2, 2022
Version of record online: June 30, 2022